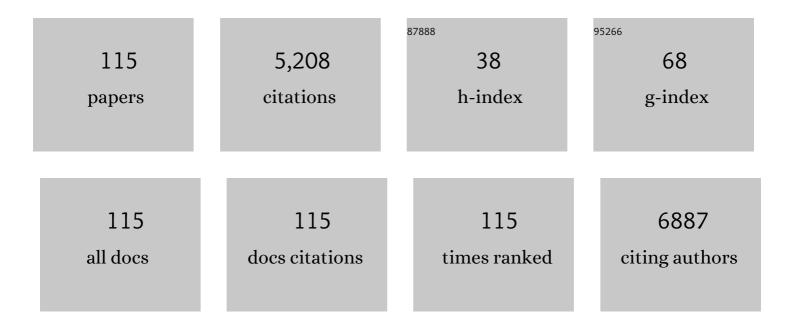
## Yantao Shi

List of Publications by Year in descending order

Source: https://exaly.com/author-pdf/5897887/publications.pdf Version: 2024-02-01



Υλητλό Shi

#	Article	IF	CITATIONS
1	The Power of Singleâ€Atom Catalysis. ChemCatChem, 2015, 7, 2559-2567.	3.7	289
2	Hole-Conductor-Free, Metal-Electrode-Free TiO <sub>2</sub> /CH <sub>3</sub> NH <sub>3</sub> PbI <sub>3</sub> Heterojunction Solar Cells Based on a Low-Temperature Carbon Electrode. Journal of Physical Chemistry Letters, 2014, 5, 3241-3246.	4.6	258
3	Low-Temperature and Solution-Processed Amorphous WO <sub><i>X</i></sub> as Electron-Selective Layer for Perovskite Solar Cells. Journal of Physical Chemistry Letters, 2015, 6, 755-759.	4.6	224
4	Insight into Perovskite Solar Cells Based on SnO <sub>2</sub> Compact Electron-Selective Layer. Journal of Physical Chemistry C, 2015, 119, 10212-10217.	3.1	209
5	Interpenetrating interfaces for efficient perovskite solar cells with high operational stability and mechanical robustness. Nature Communications, 2021, 12, 973.	12.8	189
6	In-situ liquid cell transmission electron microscopy investigation on oriented attachment of gold nanoparticles. Nature Communications, 2018, 9, 421.	12.8	171
7	Energetically favored formation of SnO2 nanocrystals as electron transfer layer in perovskite solar cells with high efficiency exceeding 19%. Nano Energy, 2017, 40, 336-344.	16.0	160
8	Low-Temperature Processed and Carbon-Based ZnO/CH <sub>3</sub> NH <sub>3</sub> PbI <sub>3</sub> /C Planar Heterojunction Perovskite Solar Cells. Journal of Physical Chemistry C, 2015, 119, 4600-4605.	3.1	153
9	Ultrarapid Sonochemical Synthesis of ZnO Hierarchical Structures: From Fundamental Research to High Efficiencies up to 6.42% for Quasi-Solid Dye-Sensitized Solar Cells. Chemistry of Materials, 2013, 25, 1000-1012.	6.7	124
10	Singleâ€Atom Catalysis in Mesoporous Photovoltaics: The Principle of Utility Maximization. Advanced Materials, 2014, 26, 8147-8153.	21.0	122
11	Flexible perovskite solar cells with simultaneously improved efficiency, operational stability, and mechanical reliability. Joule, 2021, 5, 1587-1601.	24.0	120
12	Amorphous Inorganic Electronâ€Selective Layers for Efficient Perovskite Solar Cells: Feasible Strategy Towards Roomâ€Temperature Fabrication. Advanced Materials, 2016, 28, 1891-1897.	21.0	115
13	A dual functional additive for the HTM layer in perovskite solar cells. Chemical Communications, 2014, 50, 5020.	4.1	110
14	Highly efficient telluride electrocatalysts for use as Pt-free counter electrodes in dye-sensitized solar cells. Chemical Communications, 2013, 49, 10157.	4.1	107
15	Atomically thin MoSe <sub>2</sub> /graphene and WSe <sub>2</sub> /graphene nanosheets for the highly efficient oxygen reduction reaction. Journal of Materials Chemistry A, 2015, 3, 24397-24404.	10.3	106
16	Efficient stable graphene-based perovskite solar cells with high flexibility in device assembling <i>via</i> modular architecture design. Energy and Environmental Science, 2019, 12, 3585-3594.	30.8	102
17	Improved SnO <sub>2</sub> Electron Transport Layers Solutionâ€Deposited at Near Room Temperature for Rigid or Flexible Perovskite Solar Cells with High Efficiencies. Advanced Energy Materials, 2019, 9, 1900834.	19.5	100
18	High-Performance Lead-Free Solar Cells Based on Tin-Halide Perovskite Thin Films Functionalized by a Divalent Organic Cation. ACS Energy Letters, 2020, 5, 2223-2230.	17.4	96

#	Article	IF	CITATIONS
19	Effects of 4-tert-butylpyridine on perovskite formation and performance of solution-processed perovskite solar cells. Journal of Materials Chemistry A, 2015, 3, 22191-22198.	10.3	85
20	W(Nb)O x -based efficient flexible perovskite solar cells: From material optimization to working principle. Nano Energy, 2017, 31, 424-431.	16.0	85
21	Solidâ€State Synthesis of ZnO Nanostructures for Quasiâ€Solid Dyeâ€Sensitized Solar Cells with High Efficiencies up to 6.46%. Advanced Materials, 2013, 25, 4413-4419.	21.0	72
22	Composite catalyst of rosin carbon/Fe3O4: highly efficient counter electrode for dye-sensitized solar cells. Chemical Communications, 2014, 50, 1701.	4.1	72
23	Ti1–graphene single-atom material for improved energy level alignment in perovskite solar cells. Nature Energy, 2021, 6, 1154-1163.	39.5	72
24	Bromine Doping as an Efficient Strategy to Reduce the Interfacial Defects in Hybrid Two-Dimensional/Three-Dimensional Stacking Perovskite Solar Cells. ACS Applied Materials & Interfaces, 2018, 10, 31755-31764.	8.0	65
25	CH <sub>3</sub> NH <sub>3</sub> PbI <sub>3</sub> and CH <sub>3</sub> NH <sub>3</sub> PbI <sub>3–<i>x</i>/sub&gt;CI<sub><i>x</i>/sub&gt; in Planar or Mesoporous Perovskite Solar Cells: Comprehensive Insight into the Dependence of Performance on Architecture, Journal of Physical Chemistry C, 2015, 119, 15868-15873.</sub></sub>	3.1	63
26	Surface Oxygen Vacancy-Dependent Electrocatalytic Activity of W <sub>18</sub> O <sub>49</sub> Nanowires. Journal of Physical Chemistry C, 2014, 118, 20100-20106.	3.1	62
27	Integration of Morphology and Electronic Structure Modulation on Atomic Ironâ€Nitrogen arbon Catalysts for Highly Efficient Oxygen Reduction. Advanced Functional Materials, 2022, 32, 2108345.	14.9	61
28	Carbon-based single atom catalysts for tailoring the ORR pathway: a concise review. Journal of Materials Chemistry A, 2021, 9, 24803-24829.	10.3	60
29	Transition metal selenides as efficient counter-electrode materials for dye-sensitized solar cells. Physical Chemistry Chemical Physics, 2015, 17, 28985-28992.	2.8	59
30	Interlaced W <sub>18</sub> O <sub>49</sub> nanofibers as a superior catalyst for the counter electrode of highly efficient dye-sensitized solar cells. Journal of Materials Chemistry A, 2014, 2, 4347-4354.	10.3	58
31	Melt-salt-assisted direct transformation of solid oxide into atomically dispersed FeN4 sites on nitrogen-doped porous carbon. Nano Energy, 2020, 72, 104670.	16.0	58
32	Two methoxyaniline-substituted dibenzofuran derivatives as hole-transport materials for perovskite solar cells. Journal of Materials Chemistry A, 2016, 4, 5415-5422.	10.3	56
33	The electrically conductive function of high-molecular weight poly(ethylene oxide) in polymer gel electrolytes used for dye-sensitized solar cells. Physical Chemistry Chemical Physics, 2009, 11, 4230.	2.8	54
34	Cost-effective and morphology-controllable niobium diselenides for highly efficient counter electrodes of dye-sensitized solar cells. Journal of Materials Chemistry A, 2013, 1, 11874.	10.3	52
35	Discontinuous SnO 2 derived blended-interfacial-layer in mesoscopic perovskite solar cells: Minimizing electron transfer resistance and improving stability. Nano Energy, 2017, 38, 358-367.	16.0	47
36	lron oxide nanostructures as highly efficient heterogeneous catalysts for mesoscopic photovoltaics. Journal of Materials Chemistry A, 2014, 2, 15279-15283.	10.3	45

#	Article	IF	CITATIONS
37	Room Temperature Fabrication of SnO <sub>2</sub> Electrodes Enabling Barrierâ€Free Electron Extraction for Efficient Flexible Perovskite Photovoltaics. Advanced Functional Materials, 2022, 32, .	14.9	42
38	CNT-based bifacial perovskite solar cells toward highly efficient 4-terminal tandem photovoltaics. Energy and Environmental Science, 2022, 15, 1536-1544.	30.8	39
39	Carbon-based HTL-free modular perovskite solar cells with improved contact at perovskite/carbon interfaces. Journal of Materials Chemistry C, 2020, 8, 9262-9270.	5.5	38
40	Asymmetric alkyl diamine based Dion–Jacobson low-dimensional perovskite solar cells with efficiency exceeding 15%. Journal of Materials Chemistry A, 2020, 8, 9919-9926.	10.3	38
41	Synergetic Coâ€Modulation of Crystallization and Coâ€Passivation of Defects for FAPbI <sub>3</sub> Perovskite Solar Cells. Advanced Functional Materials, 2022, 32, 2108567.	14.9	38
42	Asymmetric organic diammonium salt buried in SnO2 layer enables fast carrier transfer and interfacial defects passivation for efficient perovskite solar cells. Chemical Engineering Journal, 2022, 442, 136291.	12.7	37
43	Hexylammonium Iodide Derived Two-Dimensional Perovskite as Interfacial Passivation Layer in Efficient Two-Dimensional/Three-Dimensional Perovskite Solar Cells. ACS Applied Materials & Interfaces, 2020, 12, 698-705.	8.0	36
44	Defective MWCNT Enabled Dual Interface Coupling for Carbonâ€Based Perovskite Solar Cells with Efficiency Exceeding 22%. Advanced Functional Materials, 2022, 32, .	14.9	35
45	Atomically thin SiC nanoparticles obtained via ultrasonic treatment to realize enhanced catalytic activity for the oxygen reduction reaction in both alkaline and acidic media. RSC Advances, 2017, 7, 22875-22881.	3.6	34
46	Tea-leaf-residual derived electrocatalyst: Hierarchical pore structure and self nitrogen and fluorine co-doping for efficient oxygen reduction reaction. International Journal of Hydrogen Energy, 2018, 43, 19492-19499.	7.1	33
47	Biomass-Derived Multilayer-Graphene-Encapsulated Cobalt Nanoparticles as Efficient Electrocatalyst for Versatile Renewable Energy Applications. ACS Sustainable Chemistry and Engineering, 2019, 7, 1137-1145.	6.7	31
48	A Novel Singleâ€Atom Electrocatalyst Ti <sub>1</sub> /rGO for Efficient Cathodic Reduction in Hybrid Photovoltaics. Advanced Materials, 2020, 32, e2000478.	21.0	31
49	Morphology dependence of performance of counter electrodes for dye-sensitized solar cells of hydrothermally prepared hierarchical Cu2ZnSnS4 nanostructures. RSC Advances, 2013, 3, 23264.	3.6	29
50	Salt melt synthesis of Chlorella-derived nitrogen-doped porous carbon with atomically dispersed CoN4 sites for efficient oxygen reduction reaction. Journal of Colloid and Interface Science, 2021, 586, 498-504.	9.4	29
51	Printable fabrication of Pt-and-ITO free counter electrodes for completely flexible quasi-solid dye-sensitized solar cells. Journal of Materials Chemistry A, 2013, 1, 3932.	10.3	28
52	Onion-like graphitic carbon covering metallic nanocrystals derived from brown coal as a stable and efficient counter electrode for dye-sensitized solar cells. Journal of Power Sources, 2019, 414, 495-501.	7.8	28
53	<mml:math bold"="" xmins:mml="http://www.w3.org/1998/Math/Math/Math/Math/Math/Math/Math/Math&lt;/td&gt;&lt;td&gt;3.2&lt;/td&gt;&lt;td&gt;26&lt;/td&gt;&lt;/tr&gt;&lt;tr&gt;&lt;td&gt;54&lt;/td&gt;&lt;td&gt;mathvariant=">3 chunkmuz chunkmuzbz chunkmi High-Performance and Stable Mesoporous Perovskite Solar Cells via Well-Crystallized FA0.85MA0.15Pb(I0.8Br0.2)3. ACS Applied Materials &amp; Interfaces, 2019, 11, 2989-2996.</mml:math>	8.0	26

#	Article	IF	CITATIONS
55	[NH <sub>3</sub> (CH <sub>2</sub> ) <sub>6</sub> NH <sub>3</sub> ]PbI <sub>4</sub> as Dion–Jacobson phase bifunctional capping layer for 2D/3D perovskite solar cells with high efficiency and excellent UV stability. Journal of Materials Chemistry A, 2020, 8, 10283-10290.	10.3	26
56	Critical Role of Organoamines in the Irreversible Degradation of a Metal Halide Perovskite Precursor Colloid: Mechanism and Inhibiting Strategy. ACS Energy Letters, 2022, 7, 481-489.	17.4	26
57	Lewis base governing superfacial proton behavior of hybrid perovskite: Basicity dependent passivation strategy. Chemical Engineering Journal, 2022, 446, 137033.	12.7	26
58	Experimental investigation and theoretical exploration of single-atom electrocatalysis in hybrid photovoltaics: The powerful role of Pt atoms in triiodide reduction. Nano Energy, 2017, 39, 1-8.	16.0	25
59	An insight into the reaction mechanism of CO <sub>2</sub> photoreduction catalyzed by atomically dispersed Fe atoms supported on graphitic carbon nitride. Physical Chemistry Chemical Physics, 2021, 23, 4690-4699.	2.8	22
60	From marine plants to photovoltaic devices. Energy and Environmental Science, 2014, 7, 343-346.	30.8	21
61	Electrocatalytic properties of iron chalcogenides as low-cost counter electrode materials for dye-sensitized solar cells. RSC Advances, 2015, 5, 72553-72561.	3.6	20
62	Perovskite Solar Cell Using a Two-Dimensional Titania Nanosheet Thin Film as the Compact Layer. ACS Applied Materials & Interfaces, 2015, 7, 15117-15122.	8.0	20
63	Recent progress in interface modification for dye-sensitized solar cells. Science China Chemistry, 2010, 53, 1669-1678.	8.2	19
64	Room-temperature solution-processed amorphous NbO <sub>x</sub> as an electron transport layer in high-efficiency photovoltaics. Journal of Materials Chemistry A, 2018, 6, 17882-17888.	10.3	19
65	Understanding the Inhibition of the Shuttle Effect of Sulfides (S â‰\$) in Lithium–Sulfur Batteries by Heteroatom-Doped Graphene: First-Principles Study. Journal of Physical Chemistry C, 2020, 124, 3644-3649.	3.1	19
66	Lead-Free Flexible Perovskite Solar Cells with Interfacial Native Oxide Have >10% Efficiency and Simultaneously Enhanced Stability and Reliability. ACS Energy Letters, 2022, 7, 2256-2264.	17.4	19
67	Flexibly assembled and readily detachable photovoltaics. Energy and Environmental Science, 2017, 10, 2117-2123.	30.8	17
68	A novel composite of W <sub>18</sub> O <sub>49</sub> nanorods on reduced graphene oxide sheets based on in situ synthesis and catalytic performance for oxygen reduction reaction. RSC Advances, 2017, 7, 2051-2057.	3.6	16
69	Theoretical insight into the carrier mobility anisotropy of organic-inorganic perovskite CH3NH3PbI3. Journal of Electroanalytical Chemistry, 2018, 810, 11-17.	3.8	16
70	Unsupported Nanoporous Platinum–Iron Bimetallic Catalyst for the Chemoselective Hydrogenation of Halonitrobenzenes to Haloanilines. ACS Applied Materials & Interfaces, 2021, 13, 23655-23661.	8.0	16
71	Low-temperature sprayed carbon electrode in modular HTL-free perovskite solar cells: a comparative study on the choice of carbon sources. Journal of Materials Chemistry C, 2021, 9, 3546-3554.	5.5	16
72	High-air-flow-velocity assisted intermediate phase engineering for controlled crystallization of mixed perovskite in high efficiency photovoltaics. Journal of Materials Chemistry A, 2018, 6, 8860-8867.	10.3	15

#	Article	IF	CITATIONS
73	Pseudohalogen-Based 2D Perovskite: A More Complex Thermal Degradation Mechanism Than 3D Perovskite. Inorganic Chemistry, 2018, 57, 2045-2050.	4.0	15
74	Soft interfaces within hybrid perovskite solar cells: real-time dynamic tracking of interfacial electrical property evolution by EIS. Journal of Materials Chemistry C, 2019, 7, 8294-8302.	5.5	15
75	Hierarchical ZnO Nanostructures with Blooming Flowers Driven by Screw Dislocations. Scientific Reports, 2015, 5, 8226.	3.3	14
76	Enhanced stability of perovskite solar cells using hydrophobic organic fluoropolymer. Applied Physics Letters, 2018, 113, .	3.3	14
77	Favorable growth of well-crystallized layered hybrid perovskite by combination of thermal and solvent assistance. Journal of Power Sources, 2019, 422, 156-162.	7.8	14
78	Tuned single atom coordination structures mediated by polarization force and sulfur anions for photovoltaics. Nano Research, 2021, 14, 4025-4032.	10.4	14
79	Molecular structure simplification of the most common hole transport materials in perovskite solar cells. RSC Advances, 2016, 6, 96990-96996.	3.6	13
80	Rational design of SnO2-based electron transport layer in mesoscopic perovskite solar cells: more kinetically favorable than traditional double-layer architecture. Science China Materials, 2017, 60, 963-976.	6.3	13
81	Interfacial negative capacitance in planar perovskite solar cells: An interpretation based on band theory. Materials Research Bulletin, 2018, 107, 74-79.	5.2	13
82	Atomic Evolution of Metal–Organic Frameworks into Co–N <sub>3</sub> Coupling Vacancies by Cooperative Cascade Protection Strategy for Promoting Triiodide Reduction. Journal of Physical Chemistry C, 2021, 125, 6147-6156.	3.1	13
83	Efficient Planar Perovskite Solar Cells with Carbon Quantum Dot-Modified spiro-MeOTAD as a Composite Hole Transport Layer. ACS Applied Materials & Interfaces, 2021, 13, 56265-56272.	8.0	13
84	Boosting oxygen-reduction catalysis over mononuclear CuN2+2 moiety for rechargeable Zn-air battery. Chemical Engineering Journal, 2022, 430, 133105.	12.7	12
85	First application of bis(oxalate)borate ionic liquids (ILBOBs) in high-performance dye-sensitized solar cells. RSC Advances, 2013, 3, 12975.	3.6	11
86	New insight into the ultra-long lifetime of excitons in organic–inorganic perovskite: Reverse intersystem crossing. Journal of Energy Chemistry, 2018, 27, 1496-1500.	12.9	11
87	Molten salt as ultrastrong polar solvent enables the most straightforward pyrolysis towards highly efficient and stable single-atom electrocatalyst. Journal of Energy Chemistry, 2021, 54, 519-527.	12.9	11
88	Direct transformation of raw biomass into a Fe–N <sub>x</sub> –C single-atom catalyst for efficient oxygen reduction reaction. Materials Chemistry Frontiers, 2021, 5, 3093-3098.	5.9	11
89	Single-atom-catalyst with abundant Co–S <sub>4</sub> sites for use as a counter electrode in photovoltaics. Chemical Communications, 2021, 57, 5302-5305.	4.1	11
90	Insight into the Activity and Stability of Transition-Metal Atoms Embedded in MnO for Triiodide Reduction Reaction. ACS Sustainable Chemistry and Engineering, 2019, 7, 19303-19310.	6.7	10

4

#	Article	IF	CITATIONS
91	Imaging the Moisture-Induced Degradation Process of 2D Organolead Halide Perovskites. ACS Omega, 2022, 7, 10365-10371.	3.5	10
92	Theoretical design and experimental synthesis of counter electrode for dye-sensitized solar cells: Amino-functionalized graphene. Journal of Energy Chemistry, 2016, 25, 861-867.	12.9	9
93	Cs0.05(FA0.85MA0.15)0.95Pb(I0.85Br0.15)3 based flexible perovskite light-emitting devices with excellent mechanical bending durability. Chemical Physics Letters, 2019, 723, 33-38.	2.6	9
94	Insight into the Interfacial Elastic Contact in Stacking Perovskite Solar Cells. Advanced Materials Interfaces, 2019, 6, 1900157.	3.7	9
95	Enhancing the Interface Contact of Stacking Perovskite Solar Cells with Hexamethylenediammonium Diiodide-Modified PEDOT:PSS as an Electrode. ACS Applied Materials & Interfaces, 2020, 12, 42321-42327.	8.0	9
96	Insight into the CO2 photoreduction mechanism over 9-hydroxyphenal-1-one (HPHN) carbon quantum dots. Journal of Energy Chemistry, 2021, 52, 269-276.	12.9	9
97	Synergistically Enhanced Single-Atom Nickel Catalysis for Alkaline Hydrogen Evolution Reaction. ACS Applied Materials & Interfaces, 2022, 14, 29822-29831.	8.0	9
98	Degradation mechanism of flexible perovskite solar cells: Investigated by tracking of the heterojunction property. Materials Research Bulletin, 2020, 123, 110696.	5.2	8
99	Controlled synthesis of ZnO spindles and fabrication of composite photoanodes at low temperature for quasi-solid state dye-sensitized solar cells. Journal of Materials Chemistry, 2011, 21, 3183.	6.7	7
100	A green route and rational design for ZnO-based high-efficiency photovoltaics. Nanoscale, 2014, 6, 5093.	5.6	7
101	High electrocatalytic activity of W <sub>18</sub> O <sub>49</sub> nanowires for cobalt complex and ferrocenium redox mediators. RSC Advances, 2014, 4, 42190-42196.	3.6	7
102	Interplay between Exciton and Free Carriers in Organolead Perovskite Films. Scientific Reports, 2017, 7, 14760.	3.3	7
103	Accelerating Photogenerated Hole Tunneling through Passivation Layers <i>via</i> Reducing Interplanar Spacing for Efficient and Stable Perovskite Solar Cells. ACS Applied Materials & Interfaces, 2022, 14, 16920-16927.	8.0	6
104	Ozonization, Amination and Photoreduction of Graphene Oxide for Triiodide Reduction Reaction: An Experimental and Theoretical Study. Electrochimica Acta, 2017, 226, 10-17.	5.2	5
105	Ozone-Mediated Controllable Hydrolysis for a High-Quality Amorphous NbO <i><sub>x</sub></i> Electron Transport Layer in Efficient Perovskite Solar Cells. ACS Applied Materials & Interfaces, 2020, 12, 15194-15201.	8.0	5
106	Theoretical Insights into the Carrier Mobility Anisotropy of Organic–Inorganic Perovskite ABI3 (A =) Tj ETQq0 (	) 0 <sub>3</sub> gBT /C	veglock 10 T
107	Computational insights into the mechanism of formaldehyde detection by luminescent covalent organic framework. Journal of Molecular Modeling, 2019, 25, 248.	1.8	4

108Dual Sites of CoO Nanoparticles and Co–N<sub><i>x</i></sub> Embedded within Coal-Based Support<br/>toward Advanced Triiodide Reduction. ACS Sustainable Chemistry and Engineering, 2019, 7, 10484-10492.6.7

#	Article	IF	CITATIONS
109	Semi-Transparent and Stable Solar Cells for Building Integrated Photovoltaics: The Confinement Effects of the Polymer Gel Electrolyte inside Mesoporous Films. ACS Omega, 2019, 4, 15097-15100.	3.5	3
110	Real-Time Dynamic Observation of a Thermal and Electrical Coeffect on the Interfacial Evolution of Hybrid Perovskite Solar Cells by Electrochemical Impedance Spectroscopy. ACS Applied Energy Materials, 2020, 3, 8017-8025.	5.1	3
111	Density of photoinduced free carriers in perovskite thin films via purely optical detection. Journal of Materials Chemistry C, 2017, 5, 3283-3287.	5.5	2
112	Correlation of ETL in perovskite light-emitting diodes and the ultra-long rise time in time-resolved electroluminescence. Materials Science in Semiconductor Processing, 2018, 80, 131-136.	4.0	2
113	Role of water oxidation in the photoreduction of graphene oxide. Chemical Communications, 2019, 55, 1837-1840.	4.1	2
114	Insights into the existing form of glycolaldehyde in methanol solution: an experimental and theoretical investigation. New Journal of Chemistry, 2021, 45, 8149-8154.	2.8	2
115	Identification of glycolaldehyde, the simplest sugar, in plant systems. New Journal of Chemistry, 2022, 46, 6360-6365.	2.8	Ο